FEDSM2016-7573

ADJOINT-BASED AERODYNAMIC DESIGN OF COMPLEX AEROSPACE CONFIGURATIONS

Eric J. Nielsen[*]
Computational AeroSciences Branch
NASA Langley Research Center
Hampton, Virginia 23681
Email: Eric.J.Nielsen@nasa.gov

ABSTRACT

An overview of twenty years of adjoint-based aerodynamic design research at NASA Langley Research Center is presented. Adjoint-based algorithms provide a powerful tool for efficient sensitivity analysis of complex large-scale computational fluid dynamics (CFD) simulations. Unlike alternative approaches for which computational expense generally scales with the number of design parameters, adjoint techniques yield sensitivity derivatives of a simulation output with respect to all input parameters at the cost of a single additional simulation. With modern large-scale CFD applications often requiring millions of compute hours for a single analysis, the efficiency afforded by adjoint methods is critical in realizing a computationally tractable design optimization capability for such applications.

NOMENCLATURE

C_L	Lift coefficient
C_{M_x}, C_{M_y}	Lateral and longitudinal moment coefficients
$\mathbf{D}$	Vector of design variables
f	Objective function, also general function
i	$\sqrt{-1}$
$\mathbf{K}$	Linear elasticity coefficient matrix
L	Lagrangian function
n	Time level
$\mathbf{Q}$	Vector of volume-averaged conserved variables
$\mathbf{R}$	Vector of spatial undivided residuals
$\mathbf{X}$	Vector of grid coordinates
x	Independent variable
ε	Perturbation
θ	Blade pitch
θ_c	Collective input
θ_{1c}	Lateral cyclic input
θ_{1s}	Longitudinal cyclic input
$\mathbf{\Lambda}_f$	Flowfield adjoint variable
$\mathbf{\Lambda}_g$	Grid adjoint variable
ψ	Blade azimuth

INTRODUCTION

As access to powerful high-performance computing resources has become widespread in recent years, the use of high-fidelity physics-based simulation tools for analysis of complex aerodynamic flows becomes increasingly routine. The availability and affordability of high-fidelity analysis tools has in turn stimulated an enormous body of research aimed at applying such tools to formal design optimization of complex aerospace configurations. A survey of the relevant literature shows that optimization methods based on the Euler and Reynolds-averaged Navier-Stokes equations have indeed gained a strong foothold in the design cycle [1, 2].

For gradient-based optimization of aerospace configurations involving many design variables, the ability to generate sensitivity information at a relatively low cost is critical. Unlike forward differentiation techniques such as finite differencing [3] or direct differentiation [4], the adjoint approach performs sensitivity analysis at a cost comparable to that of a single flow solution and independent of the number of design variables [5].

Efficient evaluation of sensitivities of an output with respect to all input parameters has led to numerous applications of adjoint-based methods in various areas of research and engineering. Some of the earliest work in the field of adjoint methods for aerodynamic design can be found in the work of Pironneau [5] and Angrand [6]. Jameson developed an adjoint approach for the Euler equations in [7].

Adjoint methods can be classified into continuous and discrete variants, depending on the order in which the differentiation and discretization of the governing equations is performed.

Both approaches are used extensively in practice and the reader is referred to examples cited in the excellent overviews in [1, 2]. Based largely on the findings demonstrated in [8], a discrete adjoint approach to sensitivity analysis is used exclusively in the work presented here.

In this paper, an overview of two decades of adjoint-based algorithm development, implementation, and application at NASA Langley Research Center are presented for steady and unsteady flows. Example aerodynamic optimization problems include a high-lift application involving active flow control, a fighter aircraft with propulsion and simulated aeroelastic effects, and a rotorcraft simulation. A multidisciplinary application of the methodology is also shown for a sonic boom minimization problem. The role of adjoint methods in the field of error estimation and mesh adaptation is briefly covered, and a long-term challenge of sensitivity analysis for chaotic flows is presented.

BASELINE SOLVER

The CFD analysis solver used in the studies highlighted here has been in active development for three decades and is used to solve compressible and incompressible, steady and unsteady, inviscid, laminar, and turbulent flow equations discretized on unstructured grids [9]. The governing equations are discretized using a node-based finite-volume scheme in which the solutions are stored at the vertices of meshes comprised of any arbitrary combination of tetrahedral, prismatic, pyramidal, and hexahedral elements.

Convective fluxes are discretized in an upwind manner and second-order accuracy is achieved using an unstructured reconstruction procedure [10]. Viscous terms are formed using an approach equivalent to a Galerkin finite-element procedure [10]. For non-simplicial element types, the viscous terms are augmented with edge-based gradients to improve the h-ellipticity of the operator [11]. Several classes of temporal discretizations are available, including conventional backwards difference formulae, as well as various multistep/multistage schemes [11].

A broad range of gas dynamics models may be used, including a classical perfect gas assumption and considerably more complex models encompassing thermochemical nonequilibrium effects [12]. Available turbulence closures range from the one-equation model of Spalart and Allmaras [13] to full Reynolds stress models and hybrid RANS-LES approaches [9]. These models use spatial and temporal discretizations consistent with the mean flow.

Dynamic mesh computations are accommodated using either rigid- or deforming-mesh paradigms, or combinations thereof. The global computational domain may consist of any number of overset component meshes. Each individual mesh may be assigned a specific motion or deformation schedule; alternatively, such attributes may be driven by external models representing complementary disciplines such as aeroelasticity, six degree of freedom motion, or ablation [11]. To leverage massively parallel hardware architectures, domain decomposition approaches are combined with message passing techniques [9].

ADJOINT EQUATIONS FOR STEADY FLOWS

Consider the vector of discretized residual equations $\mathbf{R}$ for the Euler or Navier-Stokes equations as a function of the design variables $\mathbf{D}$, computational mesh $\mathbf{X}$, and flowfield variables $\mathbf{Q}$. Given a steady-state solution of the form $\mathbf{R}(\mathbf{D}, \mathbf{Q}, \mathbf{X}) = 0$, a Lagrangian function L can be defined as

$$L(\mathbf{D}, \mathbf{Q}, \mathbf{X}, \mathbf{\Lambda}_f, \mathbf{\Lambda}_g) = f(\mathbf{D}, \mathbf{Q}, \mathbf{X}) + \mathbf{\Lambda}_f^T \mathbf{R}(\mathbf{D}, \mathbf{Q}, \mathbf{X}), \quad (1)$$

where $f(\mathbf{D}, \mathbf{Q}, \mathbf{X})$ represents an objective function of interest and $\mathbf{\Lambda}_f$ represents a vector of Lagrange multipliers, or adjoint variables, corresponding to the governing flow equations. The sensitivity $\frac{df}{d\mathbf{D}}$ is computed by differentiating Eq. 1 with respect to $\mathbf{D}$. Regrouping terms to collect the coefficients of $\frac{d\mathbf{Q}}{d\mathbf{D}}$, and equating those coefficients to zero yields the adjoint equation for steady flow,

$$\left[\frac{\partial \mathbf{R}}{\partial \mathbf{Q}} \right]^T \mathbf{\Lambda}_f = - \left[\frac{\partial f}{\partial \mathbf{Q}} \right]^T. \quad (2)$$

This linear system of equations is independent of $\mathbf{D}$ and is often solved in a pseudo-time marching fashion analogous to the CFD analysis procedure. In this manner, the expense associated with solving the adjoint equations is similar to that of the analysis problem. Moreover, if the solution algorithm is itself carefully constructed in a discretely adjoint manner, the asymptotic convergence rates of the two systems are guaranteed to be identical [14].

Upon solution of Eq. 2, $\frac{dL}{d\mathbf{D}}$ takes the following form,

$$\frac{dL}{d\mathbf{D}} = \frac{\partial f}{\partial \mathbf{D}} + \mathbf{\Lambda}_f^T \left[\frac{\partial \mathbf{R}}{\partial \mathbf{D}} \right] + \left[\frac{\partial f}{\partial \mathbf{X}} \right] \left[\frac{d\mathbf{X}}{d\mathbf{D}} \right] + \mathbf{\Lambda}_f^T \left[\frac{\partial \mathbf{R}}{\partial \mathbf{X}} \right] \left[\frac{d\mathbf{X}}{d\mathbf{D}} \right]. \quad (3)$$

This expression can be used to evaluate the sensitivities of interest. However, an explicit evaluation of the term $\frac{d\mathbf{X}}{d\mathbf{D}}$ may become prohibitively expensive. This term represents the sensitivities of the mesh point locations to design parameters such as shape variables. For mesh deformations obeying the linear elasticity relations of solid mechanics, the following equation holds

$$\mathbf{K}\mathbf{X} = \mathbf{X}_{surf}, \quad (4)$$

where $\mathbf{K}$ is an elasticity matrix based on local mesh properties and $\mathbf{X}_{surf}$ is the vector of surface mesh coordinates complemented by zeros for all interior coordinates [11, 15]. By differentiating Eq. 4 with respect to $\mathbf{D}$,

$$\mathbf{K} \left[\frac{d\mathbf{X}}{d\mathbf{D}} \right] = \frac{d\mathbf{X}_{surf}}{d\mathbf{D}}, \quad (5)$$

a linear system of equations is obtained for the desired quantity $\frac{d\mathbf{X}}{d\mathbf{D}}$. Unfortunately Eq. 5 must be solved for each geometric parameter in $\mathbf{D}$. In practice, the cost of solving Eq. 4 (or equivalently, Eq. 5) for highly anisotropic meshes can be as much as

30% of the computational cost associated with solving the flow equations [15]. Thus, for even moderate numbers of geometric design parameters, explicit evaluation of the term $\frac{\partial \mathbf{X}}{\partial \mathbf{D}}$ can be quite costly, and can even dominate the overall design computation.

In [16], it was shown that an adjoint approach could be used to account for the mesh sensitivity terms by extending the Lagrangian function in Eq. 1 to include the residual of the mesh deformation equations as an additional constraint:

$$L(\mathbf{D},\mathbf{Q},\mathbf{X},\mathbf{\Lambda}_f,\mathbf{\Lambda}_g) = f(\mathbf{D},\mathbf{Q},\mathbf{X}) \\ + \mathbf{\Lambda}_f^T \mathbf{R}(\mathbf{D},\mathbf{Q},\mathbf{X}) + \mathbf{\Lambda}_g^T (\mathbf{X}_{surf} - \mathbf{KX}) \quad (6)$$

Here, an additional adjoint variable, $\mathbf{\Lambda}_g$, associated with the mesh deformation has been introduced. Differentiating Eq. 6 with respect to $\mathbf{D}$ and seeking to eliminate the coefficient of $\frac{d\mathbf{X}}{d\mathbf{D}}$ yields an adjoint equation for the mesh deformation,

$$\mathbf{K}^T \mathbf{\Lambda}_g = \left[\frac{\partial f}{\partial \mathbf{X}} \right]^T + \left[\frac{\partial \mathbf{R}}{\partial \mathbf{X}} \right]^T \mathbf{\Lambda}_f. \quad (7)$$

After solving Eq. 2 for $\mathbf{\Lambda}_f$, Eq. 7 can be solved for $\mathbf{\Lambda}_g$ at an expense equivalent to that of solving Eq. 4. In this manner, the effects of mesh sensitivities can be formally included at an expense independent of the number of design variables. This formulation was enabling for efficient large-scale sensitivity analysis and design using a discrete adjoint formulation.

Once solutions for $\mathbf{\Lambda}_f$ and $\mathbf{\Lambda}_g$ have been determined, the remaining terms in $\frac{dL}{d\mathbf{D}}$ are as follows,

$$\frac{dL}{d\mathbf{D}} = \frac{\partial f}{\partial \mathbf{D}} + \mathbf{\Lambda}_f^T \left[\frac{\partial \mathbf{R}}{\partial \mathbf{D}} \right] + \mathbf{\Lambda}_g^T \left[\frac{d\mathbf{X}_{surf}}{d\mathbf{D}} \right]. \quad (8)$$

The first two terms on the right hand side of Eq. 8 represent the explicit dependence of the objective function and residual vector on $\mathbf{D}$. For shape design variables, these terms are identically zero, and Eq. 8 reduces to an inexpensive matrix-vector product over the parameterized surface meshes.

To summarize, the CFD analysis problem can be cast as three steps: (1) Given $\mathbf{D}$, determine the corresponding surface grid, $\mathbf{X}_{surf}$; (2) Solve the mesh deformation equations based on the new surface grid to obtain $\mathbf{X}$; and (3) Solve the flowfield equations to determine the relevant objective function f. The adjoint-based sensitivity analysis follows three similar steps, albeit in reverse fashion: (1) Solve the flowfield adjoint equations, Eq. 2, for $\mathbf{\Lambda}_f$; (2) Solve the mesh adjoint equations, Eq. 7, for $\mathbf{\Lambda}_g$; and (3) Perform an explicit matrix-vector product over the surface to obtain the desired sensitivities $\frac{dL}{d\mathbf{D}}$. In this manner, a discretely-consistent sensitivity analysis may be performed at a cost equivalent to that of the baseline CFD analysis problem and independent of the dimension of $\mathbf{D}$.

ADJOINT EQUATIONS FOR UNSTEADY FLOWS

A similar approach can be used to derive the adjoint equations for unsteady flows; however, this procedure is beyond the

current scope. Instead, the reader is referred to [17], which presents a detailed derivation of the unsteady form of the adjoint equations for a family of backward-difference temporal schemes. Terms necessary for dynamic, deforming, parent-child, and overset mesh formulations are also included.

IMPLEMENTATION

A broad range of objective functions is available. These include conventional surface integral quantities such as aerodynamic coefficients as well as the lift-to-drag ratio, power, and target pressure distributions for inverse design. Application-specific metrics such as equivalent area and off-body pressure distributions for sonic boom mitigation and the figure of merit function for rotors in hover are also included. Note that any of these functions may also be used as constraint functions in the optimization problem; the implementation simply performs sensitivity analysis for the specified functions regardless of their role in the design problem statement.

Design variables may include global inputs such as the freestream Mach number, angles of attack or sideslip, and noninertial rotation rates. For shape design, any geometric parameterization of the surface mesh $\mathbf{X}_{surf}(\mathbf{D})$ may be used, provided the Jacobian $\frac{\partial \mathbf{X}_{surf}}{\partial \mathbf{D}}$ is also supplied. For unsteady flows, kinematic parameters such as rotation and translation origins, vectors, and rates may be used as design parameters. The user may also designate inputs to a user-supplied kinematics routine, such as spline coefficients, as design parameters. In this manner, very general kinematic schedules such as that of a biologically-inspired device [18] may be prescribed and optimized.

To perform an adjoint-based sensitivity analysis, the discrete residual vector $\mathbf{R}$ and the objective function f must be differentiated with respect to the flowfield solution $\mathbf{Q}$ and the mesh coordinates $\mathbf{X}$. In the current implementation, this differentiation is done entirely by hand and verified through an independent approach described in a subsequent section.

Equation 2 is solved in a pseudo-time marching fashion using a defect correction technique, which is directly analogous to that of the baseline CFD analysis [17]. The matrix-vector product $\left[\frac{\partial \mathbf{R}}{\partial \mathbf{Q}} \right]^T \mathbf{\Lambda}_f$ may be evaluated on a term-by-term basis for memory efficiency or stored explicitly for faster execution. An arbitrary number of objective functions f may be prescribed; unique adjoint solutions for each function are efficiently computed in a single execution by accommodating multiple right-hand side vectors in the solution of Eq. 2. In this manner, the computational overhead associated with constructing $\frac{\partial \mathbf{R}}{\partial \mathbf{Q}}$ and the approximate Jacobian matrices used by the defect correction scheme are amortized over all user-specified functions [14].

Equation 7 is solved using a preconditioned Generalized Minimum Residual algorithm [19], in which the linear elasticity coefficient matrix $\mathbf{K}^T$ is stored explicitly. Following the solution of Eqs. 2 and 7, Eq. 8 is evaluated to compute the desired sensitivities.

Challenges for Unsteady Flows

Unique challenges arise when applying adjoint-based sensitivity analysis to unsteady flows. These include the increased expense associated with time-dependent computations, big data requirements, and in the case of eddy-resolving analysis schemes such as large-eddy or direct numerical simulations, the effects of chaotic dynamics. The first two challenges are discussed here, while the third will be addressed in a subsequent section.

Expense   For steady flows, the Jacobian matrix $\left[\frac{\partial \mathbf{R}}{\partial \mathbf{Q}}\right]^T$ is typically formed once and stored as an explicit matrix to minimize the time required to solve Eq. 2. Although not shown here, the time-dependent form of the adjoint equations requires the linearizations of $\mathbf{R}$ with respect to $\mathbf{Q}$ and $\mathbf{X}$ to be evaluated at each physical time step of the solution.

Big Data   The time-dependent adjoint equations must be solved in reverse physical time. This requires that the complete unsteady flowfield solution be available during reverse integration. For dynamic grid simulations, the mesh coordinates must also be available. This storage requirement can amount to many terabytes of data for realistic applications.

The flowfield solution and mesh coordinates are stored to disk at the conclusion of each physical time step of the baseline CFD analysis using a strategy designed to minimize file system overhead. The approach is based on a massively parallel paradigm, in which each processor writes to its own unformatted direct-access file at each time step. The data writes are buffered using an asynchronous paradigm, so that execution of floating point operations for the subsequent time step may proceed simultaneously. This approach is described and evaluated in [20] and has been found to scale well to several thousand processors using a parallel file system. During the time-dependent adjoint solution procedure, data are loaded from disk using a reverse paradigm, such that data required for the solution at time level $n-1$ are preloaded during the computations for time level n. Although not shown, the sensitivity derivatives computed from the time-dependent form of Eq. 8 are collected during the reverse-time solution of the adjoint equations, so no disk space is required to store the adjoint solutions.

Verification Procedure

Historically, finite differencing has been extensively used to verify the accuracy of the linearization matrices required by an adjoint implementation. However, the shortcomings of this approach are well-known and include the difficulty in selecting an appropriate step size and the accuracy limitations associated with finite truncation error. These drawbacks typically limit the agreement that may be obtained with analytic derivatives to 4-5 digits of accuracy.

A simple, yet extremely powerful mathematical expression for the derivative of a real-valued function $f(x)$ based on the use of complex variables was originally introduced in [21, 22] and resurfaced in [23]. Using this formulation, an expression for the derivative $f'(x)$ may be found by expanding the function in a complex-valued Taylor series, using an imaginary perturbation $i\varepsilon$:

$$f'(x) = \frac{Im\left[f(x+i\varepsilon)\right]}{\varepsilon} + O(\varepsilon^2). \tag{9}$$

The primary advantage of this method is that true second-order accuracy may be obtained by selecting a step size without concern for subtractive cancellation errors typically present in real-valued Frechet derivatives. For computations reported here, the imaginary step size is chosen to be 10^{-50}, which highlights the robustness of the approach.

Though seldom referenced in the literature, the earliest known use of the complex-variable methodology for large-scale simulation was reported in [24, 25]. Here, the CFD analysis solver described in the current work was coupled with a finite-element structural solver and the complex-variable approach was used to compute sensitivities of aerostructural simulations. Today, the technique is widespread not only within the CFD community, but across a broad range of computational disciplines including bioprocess modeling [26], material science [27], chemistry [28], thermal analysis [29], geophysics [30], structural analysis [31], solid mechanics [32], systems and control [33], and others.

The role of Eq. 9 in verifying adjoint implementations cannnot be overstated. In early work in which verification studies relied on real-valued finite differences such as [34], the accuracy of linearizations could only be demonstrated to approximately 0.01%. The complex-variable methodology revolutionized the process of adjoint code development, allowing an implementation to be systematically verified to machine precision, which is now standard practice [17]. Through the use of an automated scripting procedure outlined in [35], a complex-variable capability can be immediately recovered at any time for the analysis solver used here.

While the complex-variable formulation is invaluable for development and verification purposes, the method represents a forward mode of differentation and is therefore generally not used directly for aerodynamic design applications characterized by many variables. However, a novel application of the approach was used to generate adjoint operators in [36]. Here, complex-valued residual and objective function evaluations were performed on local stencils to efficiently generate partial derivatives used to assemble complete Jacobian matrices for the adjoint equations. The approach was used to demonstrate efficient adjoint-based sensitivity analysis for complex governing equation sets involving chemical nonequilibrium effects, for which hand-differentiation would be extremely cumbersome.

DESIGN APPLICATIONS

Several unsteady applications are included here as examples of the current adjoint-based design capability. The governing equations for each application are the compressible Reynolds-averaged Navier-Stokes equations. Each of the cases shown was executed on a few thousand computational cores and typically required $O(1)$ day of wall-clock time to complete. Several widely-available nonlinear programming packages have been used to perform the optimizations, and any constraints specified have
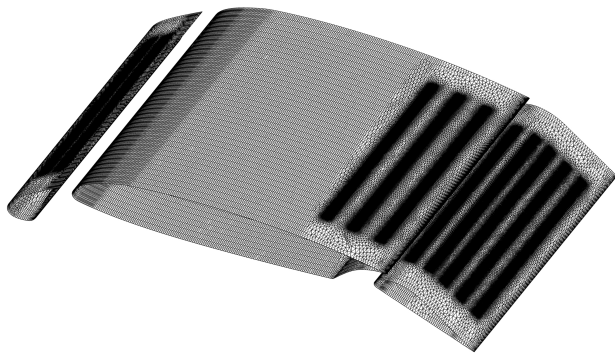
FIGURE 1. SURFACE MESH FOR HIGH-LIFT WING SECTION, WHERE REGIONS OF CLUSTERING INDICATE JET ORIFICES. TAKEN FROM [20].
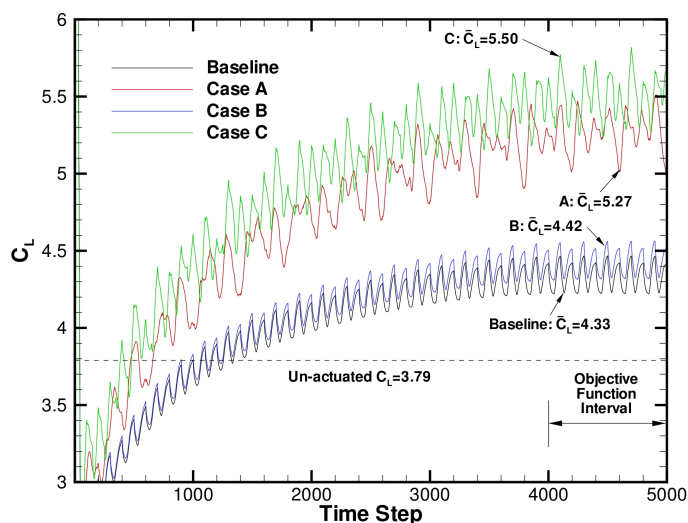
FIGURE 2. UNSTEADY LIFT PROFILES FOR THE BASELINE AND OPTIMIZED HIGH-LIFT WING CONFIGURATION. TAKEN FROM [20].

been posed in an explicit fashion. The examples are presented in order of increasing complexity and the reader is encouraged to consult the stated references for further details on each of the simulations shown. The governing equations are the compressible Reynolds-averaged Navier-Stokes equations.

Design of a High-Lift Wing Section with Active Flow Control

Adjoint-based design of a high-lift wing section with an active flow control system has been performed in [20]. The geometry used in this study has been generated by extruding a three-element airfoil section taken from [37] in the spanwise direction. A series of ten rectangular jet orifices are located along the chord of the airfoil, with two orifices located on the slat, three located on the main element, and the remaining five orifices located on the flap. An unsteady sinusoidal blowing condition is applied at the base of each slot to increase the lift produced by the baseline geometry. The computational mesh consists of 50,870,813 tetrahedral elements and the surface mesh is shown in Fig. 1. The freestream Mach number is 0.1, the angle of attack is 19 deg, and the Reynolds number is 3 million based on the chord of the

FIGURE 3. MODIFIED F-15 WITH ENGINE DUCT GEOMETRY. TAKEN FROM [38].

wing.

The objective function is to maximize the time-averaged value of the lift coefficient. The velocity magnitude, actuation frequency, actuation phase, chordwise location, and incidence angle for each individual jet actuator are used as design variables. The airfoil shape is parameterized using several B-splines, and the displacements of each B-spline control point normal to the surface are also used as design variables. Finally, the horizontal, vertical, and rotational displacement of each body may also vary during the optimization.

Several approaches to the optimization problem have been evaluated and the unsteady lift histories are shown in Fig. 2. In the absence of any flow control, the steady-state lift coefficient for the baseline geometry is 3.79. Using the baseline actuation parameters, the time-averaged value of the lift coefficient measured over the final 1,000 time steps is 4.33. As indicated in the figure, the optimization procedure labeled as Case C results in a configuration that yields a time-averaged lift coefficient of 5.50, an increase of 27% relative to the lift obtained with non-optimized actuation.

Design of a Modified F-15 Configuration with Propulsion and Simulated Aeroelastic Effects

This example taken from [38] uses a deforming grid approach to simulate aeroelastic motion of the modified F-15 fighter jet configuration known as NASA research aircraft 837, shown in Fig. 3.[1] The computational model assumes half-plane symmetry in the spanwise direction. The grid consists of 27,344,343 tetrahedral elements and includes detailed features of the external airframe as well as the internal ducting upstream of the engine fan face and the plenum/nozzle combination downstream of the turbine. For the current test, the freestream Mach number is 0.90, the angle of attack is 0 deg, and the Reynolds number based on the mean aerodynamic chord (MAC) is 1×10^6.

The prescribed grid motion consists of 5 Hz 0.3 deg oscillatory rotations of the canard, wing, and tail surfaces about their root chord lines, with the wing oscillations 180 deg out of phase

---

[1]Data available online at http://www.nasa.gov/centers/dryden/aircraft/F-15B-
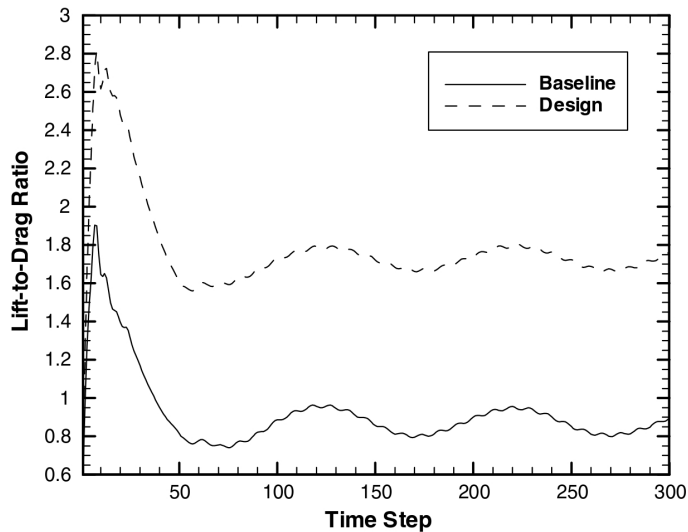
FIGURE 4. LIFT-TO-DRAG RATIO FOR MODIFIED F-15 BE-FORE AND AFTER DESIGN OPTIMIZATION. TAKEN FROM [38].
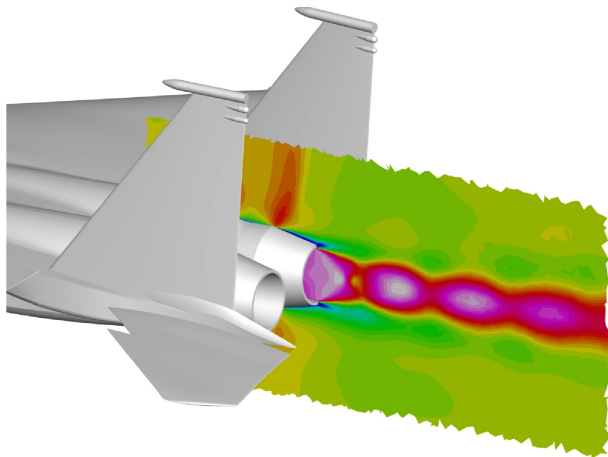

**FIGURE 5**. CROSS-SECTION OF ENGINE PLUME CONTOURS FOR MODIFIED F-15. TAKEN FROM [38].

with the canard and tail motion. In addition, the main wing is also subjected to a 5 Hz oscillatory twisting motion for which the amplitude decays linearly from 0.5 deg at the wing tip to 0 deg at the wing root and takes place about the quarter-chord line. This composite motion results in a maximum wing tip deflection of approximately 1.3% MAC.

The unsteady lift-to-drag ratio (L/D) for the baseline con-figuration undergoing the specified motion for 300 time steps is shown as the solid line in Fig. 4. The L/D behavior begins to exhibit a periodic response after approximately 100 time steps. The high-frequency oscillations in the profile are believed to be due to a small unsteadiness in the engine plume shown in Fig. 5; this behavior is also present when the mesh is held fixed.

The objective function for the design problem is to maxi-mize L/D between time steps 201 and 300. Design variables include thickness and camber distributions for the canard, wing, and tail surfaces. Thinning of the geometry is not permitted, and other bound constraints are chosen to avoid nonphysical geome-tries.
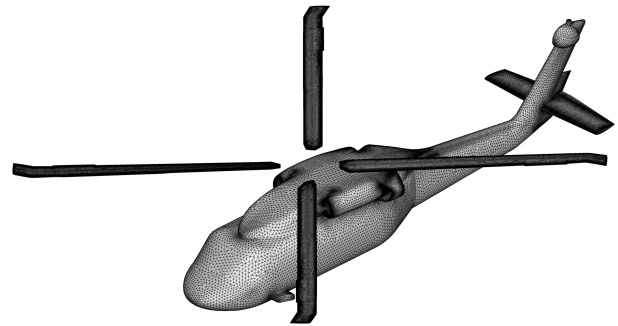
**FIGURE 6**. SURFACE MESH FOR UH-60A CONFIGURATION. TAKEN FROM [17].
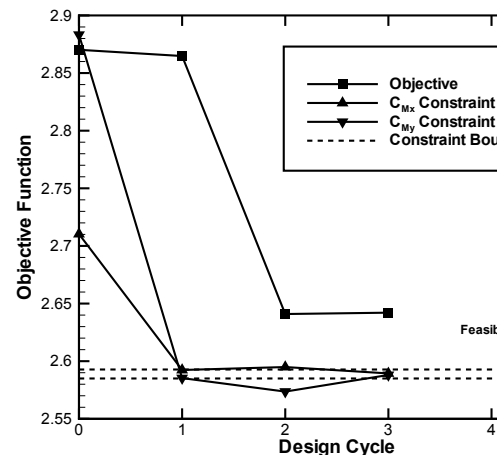
FIGURE 7. CONVERGENCE OF THE OBJECTIVE FUNCTION AND CONSTRAINTS FOR THE UH-60A CONFIGURATION. TAKEN FROM [17].

The final L/D profile is included as the dashed line in Fig. 4. Although not shown, the design procedure has increased the thickness of the wing and canard, as well as the camber across all three elements. The trailing edges of each surface have also been deflected in a downward fashion.

Constrained Design of a UH-60A Blackhawk Helicopter

To demonstrate the adjoint-based design capability for sim-ulations involving dynamic overset grids, an optimization of a UH-60A Blackhawk helicopter has been presented in [17]. Here, the composite overset grid system consists of four blade compo-nent grids and a single component grid containing the fuselage and outer extent of the computational domain. The complete grid system contains 54,642,499 tetrahedral elements and the surface meshes are shown in Fig. 6.

The simulation is based on a forward flight condition with a blade tip Mach number equal to 0.6378 and a Reynolds number of 7.3 million based on the blade tip chord. The advance ratio is 0.37 and the angle of attack is 0 deg. The rotor blades are subjected to a time-dependent pitching motion that is modeled as a child of the azimuthal rotation and is governed by a sinusoidal
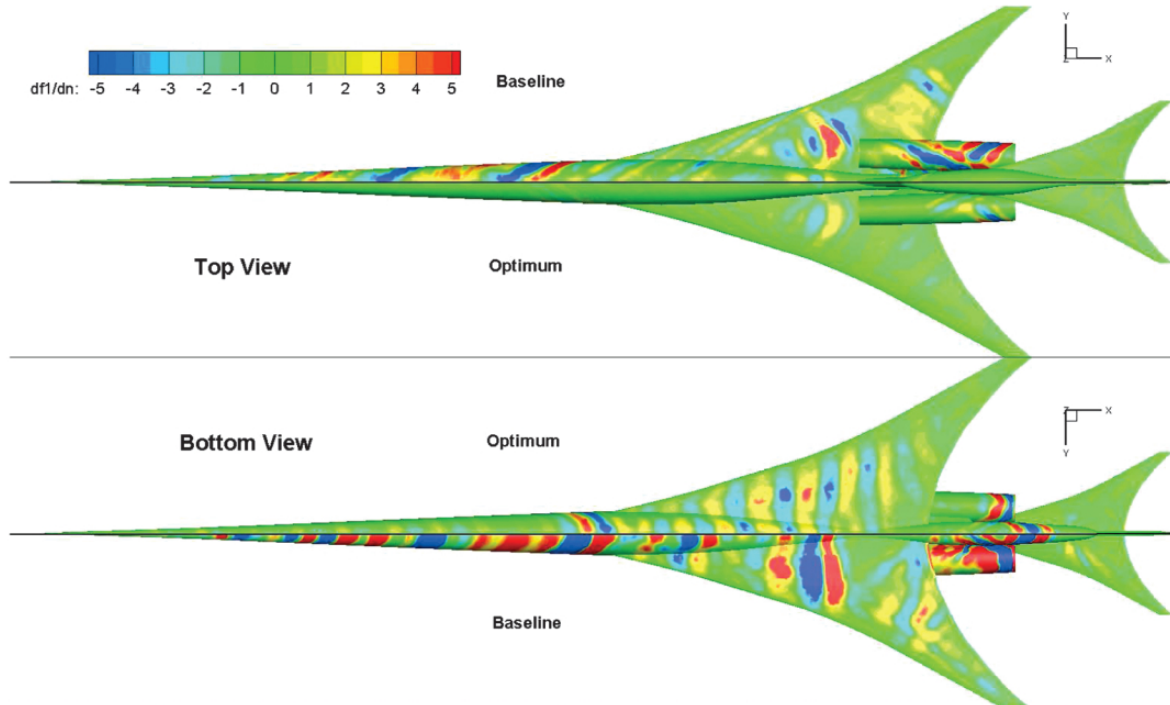
FIGURE 8.   SENSITIVITY OF GROUND-BASED NOISE METRIC TO SURFACE PERTURBATIONS IN THE NORMAL DIRECTION FOR A SUPERSONIC VEHICLE CONCEPT, BEFORE AND AFTER OPTIMIZATION. TAKEN FROM [39].

variation based on collective and cyclic control inputs:

$$\theta = \theta_c + \theta_{1c}cos\psi + \theta_{1s}sin\psi \qquad (10)$$

Here, θ is the current blade pitch setting, ψ is the current azimuth position for the blade, θ_c represents the collective control input, and θ_{1c} and θ_{1s} are the lateral and longitudinal cyclic control inputs, respectively. All three control inputs are set to 0 deg at the baseline condition; i.e., the vehicle is initially untrimmed.

The objective for the current test case is to maximize the lift acting on the vehicle while satisfying explicit constraints on the lateral and longitudinal moments such that the final result is a trimmed flight condition. The initial mean value of the unsteady lift profile is 0.023. The design variables consist of 64 shape parameters describing the rotor blades, including 32 thickness and 32 camber variables. While the camber is allowed to increase or decrease, no thinning of the blade is allowed. In addition, the control variables θ_c, θ_{1c}, and θ_{1s} are also used as design variables. These control angles are allowed to vary as much as ±7 deg.

Figure 7 shows the convergence of the objective function and constraints after three design cycles. The optimization procedure quickly locates a feasible region in the design space based on the two moment constraints, and the value of the objective function is successfully reduced. The mean value of the final unsteady lift profile has been substantially increased to a value of 0.103, and the vehicle is trimmed for level flight within the requested tolerance.

OTHER USES

The adjoint-based capability described here has also had impact in areas beyond fluid design problems. Examples of its application to multidisciplinary optimization and error estimation and mesh adaptation are briefly described here.

Multidisciplinary Design Problems

While many applications of adjoint-based sensitivity analysis and design have been demonstrated for a broad range of CFD simulations, a similar approach can also be formulated across disciplines. In this manner, the algorithmic efficiency of adjoint methods can be brought to bear on multidisciplinary design problems previously considered computationally intractable.

Such an approach has recently been applied to coupled simulations aimed at sonic boom mitigation. In this application, the designer is interested in the impact of pressure disturbances generated by aircraft operating several miles above an observer at ground level. In general, it is computationally infeasible to resolve the entire domain using a traditional CFD method. Instead, high-fidelity CFD simulations are typically used to predict the highly nonlinear flowfield only in the immediate vicinity of the vehicle. This solution for the near-field pressure distribution is then propagated to a ground-based observer using inexpensive propagation techniques. Finally, the ground-level pressure distribution can be converted to a noise metric suitable for trade studies.

In [39], an adjoint-based sensitivity analysis procedure has been applied to a sonic boom prediction methodology using CFD-based simulations for near-field analysis, a one-dimensional Burgers equation for atmospheric propagation, and noise-processing techniques to ultimately determine human im-

pact metrics. To perform a rigorous sensitivity analysis of this coupled system, the sensitivities of the ground-based noise metrics with respect to the propagated pressure signal are first determined. These sensitivities are then propagated from ground level to the location of the CFD interface using a discrete adjoint formulation for the atmospheric propagation. Finally, these sensitivities at the interface with the CFD mesh provide a forcing function for the CFD adjoint problem, ultimately enabling the computation of discretely-consistent sensitivities of ground-based noise metrics with respect to geometric (or any other) parameters characterizing the aircraft configuration. Rather than relying on conventional heuristic trial-and-error methods, aircraft designers may instead apply the adjoint-based approach to perform rigorous optimization of vehicle concepts using ground-based noise metrics.

Figure 8 shows the sensitivity of the ground-based objective function to surface perturbations normal to the aircraft outer mold line. Results are shown for the vehicle upper and lower surfaces before and after the optimization. The sensitivities on the fuselage, wing, tail, and nacelle surfaces have been substantially reduced by the design procedure. For this case, the A-weighted and perceived loudness metrics computed at ground level were reduced from 65.2 dBA to 59.8 dBA and 79.7 dB to 74.9 dB, respectively.

Efforts are currently focused on similar integration strategies for disciplinary models such as structures and materials, propulsion, multibody dynamics, acoustics, flight control, and optics.

Error Estimation and Mesh Adaptation

The adjoint-based methodology described here has also enabled a rigorous approach to error estimation and mesh adaptation for CFD simulations [40]. By inspection of Eq. 2, it is apparent that the adjoint variable $\mathbf{\Lambda}_f$ represents the sensitivity of the objective function to local truncation error. This sensitivity vector can be used along with a measure of the local truncation error to provide estimates of local contributions to the error in computing the objective function f. Furthermore, a direct relationship between local grid spacing requirements and the desired solution accuracy for f can be established. In this manner, mesh adaptation can be systematically guided by the requirements of the underlying partial differential equations. This approach has proven vastly superior to feature-based adaptation processes relying on heuristic measures such as solution gradients, which often produce visually attractive results but lack the mathematical rigor.

An example of adjoint-based mesh adaptation taken from [41] is included in Fig. 9. Here, the mesh for an engine nozzle operating in a supersonic external flow has been adapted to reduce the error in computing an off-body pressure signal for sonic boom analysis. The adjoint-based procedure has implicitly determined the regions of the domain critical to computing the function of interest, refining the mesh in the vicinity of several shock structures and smooth expansion regions as well as the shear layers propagating downstream from the cowl and plug surfaces.
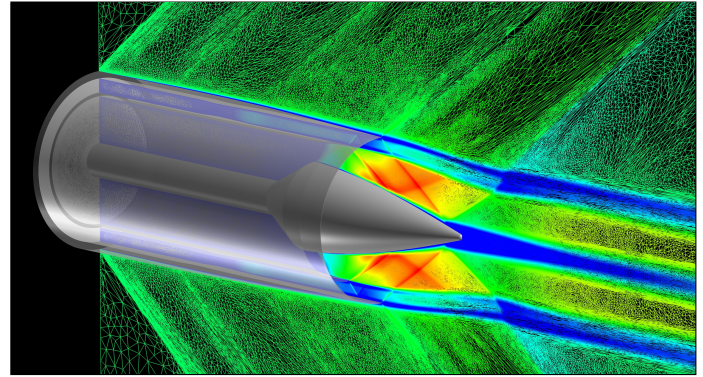
FIGURE 9. ADJOINT-BASED MESH ADAPTATION FOR AN ENGINE NOZZLE IN A SUPERSONIC EXTERNAL FLOW. TAKEN FROM [41].

AN EMERGING CHALLENGE: CHAOS

Gradient-based sensitivity analysis has proven to be an enabling technology for many applications, including design of aerospace vehicles. However, conventional sensitivity analysis methods break down when applied to long-time averages of chaotic systems. This breakdown is a serious limitation because many aerospace applications involve physical phenomena that exhibit chaotic dynamics, most notably high-resolution large-eddy and direct numerical simulations of turbulent aerodynamic flows.

The breakdown of conventional sensitivity analysis can be traced to certain fundamental properties of chaotic systems. Specifically, Lorenz's butterfly effect implies that the time evolution of a chaotic system is highly sensitive to initial conditions [42]. A small perturbation to initial conditions may grow exponentially over time, resulting in large differences in instantaneous solutions. This high sensitivity is observed for all chaotic systems.

A recently proposed methodology, Least Squares Shadowing (LSS) [43], avoids this breakdown and advances the state of the art in sensitivity analysis for chaotic flows. This method transforms the conventional time-marching problem to a coupled space-time system. The first application of LSS to a chaotic flow simulated with a large-scale CFD solver was presented in [44]. The LSS sensitivity for a chaotic two-dimensional inviscid flow was verified and shown to be accurate, but the computational cost was estimated to be at least five orders of magnitude more than the cost of the baseline analysis problem.

The LSS approach represents the most efficient sensitivity analysis method for chaotic flows developed to date; however, its application remains prohibitively expensive for practical aerospace simulations. Revolutionary breakthroughs in solution technologies for LSS sensitivity analysis as well as increased availability of leadership-class computing resources are needed to enable practical high-fidelity design for aerospace applications involving chaotic flows.

ACKNOWLEDGMENTS

REFERENCES

[1] Newman III, J., Taylor III, A., Barnwell, R., Newman, P., and Hou, G.-W., 1999. "Overview of Sensitivity Analysis and Shape Optimization for Complex Aerodynamic Configurations". *AIAA Journal of Aircraft, 36*(1), pp. 87–96.

[2] Peter, J., and Dwight, R., 2010. "Numerical Sensitivity Analysis for Aerodynamic Optimization: A Survey of Approaches". *Computers and Fluids, 39*(3), pp. 373–391.

[3] Hicks, R., and Henne, P., 1978. "Wing Design by Numerical Optimization". *AIAA Journal of Aircraft, 15*(7), pp. 407–412.

[4] Baysal, O., and Eleshaky, M., 1991. "Aerodynamic Sensitivity Analysis Methods for the Compressible Euler Equations". *Journal of Fluids Engineering, 113*(4), pp. 681–688.

[5] Pironneau, O., 1973. "On Optimum Profiles in Stokes Flow". *Journal of Fluid Mechanics, 59*(1), pp. 117–128.

[6] Angrand, F., 1983. "Optimum Design for Potential Flows". *International Journal of Numerical Methods in Fluids, 3*, pp. 265–282.

[7] Jameson, A., 1988. "Aerodynamic Design via Control Theory". *Journal of Scientific Computing, 3*, pp. 233–260.

[8] Anderson, W. K., and Venkatakrishnan, V., 1999. "Aerodynamic Design Optimization on Unstructured Grids with a Continuous Adjoint Formulation". *Computers and Fluids, 28*(4), pp. 443–480.

[9] Biedron, R. T., Carlson, J.-R., Derlaga, J. M., Gnoffo, P. A., Hammond, D. P., Jones, W. T., Kleb, W. L., Lee-Rausch, E. M., Nielsen, E. J., Park, M. A., Rumsey, C. L., Thomas, J. L., and Wood, W. A., 2015. "FUN3D Manual: 12.8". NASA/TM-2015-218807.

[10] Anderson, W. K., and Bonhaus, D. L., 1994. "An Implicit Upwind Algorithm for Computing Turbulent Flow on Unstructured Grids". *Computers and Fluids, 23*(1), pp. 1–21.

[11] Biedron, R. T., and Thomas, J. L., 2009. "Recent Enhancements to the FUN3D Flow Solver for Moving-Mesh Applications". AIAA 2009-1360.

[12] Gnoffo, P. A., and White, J. A., 2004. "Computational Aerothermodynamic Simulation Issues on Unstructured Grids". AIAA 2004-2371.

[13] Spalart, P. R., and Allmaras, S. R., 1994. "A One-Equation Turbulence Model for Aerodynamic Flows". *La Recherche Aerospatiale, 1*(1), pp. 5–21.

[14] Nielsen, E. J., Lu, J., Park, M. A., and Darmofal, D. L., 2004. "An Implicit, Exact Dual Adjoint Solution Method for Turbulent Flows on Unstructured Grids". *Computers and Fluids, 33*(9), pp. 1131–1155.

[15] Nielsen, E. J., and Anderson, W. K., 2002. "Recent Improvements in Aerodynamic Design Optimization on Unstructured Meshes". *AIAA Journal, 40*(6), pp. 1155–1163.

[16] Nielsen, E. J., and Park, M. A., 2006. "Using an Adjoint Approach to Eliminate Mesh Sensitivities in Computational Design". *AIAA Journal, 44*(5), pp. 948–953.

[17] Nielsen, E. J., and Diskin, B., 2013. "Discrete Adjoint-Based Design for Unsteady Turbulent Flows on Dynamic Overset Unstructured Grids". *AIAA Journal, 51*(6), pp. 1355–1373.

[18] Jones, M. "CFD Analysis and Design Optimization of Flapping Wing Flows". PhD Thesis, North Carolina A&T State University, Greensboro, NC, June 2013.

[19] Saad, Y., and Schultz, M. H., 1986. "GMRES: A Generalized Minimum Residual Algorithm for Solving Nonsymmetric Linear Systems". *SIAM Journal on Scientific and Statistical Computing, 7*(3), pp. 856–869.

[20] Nielsen, E. J., and Jones, W. T., 2011. "Integrated Design of an Active Flow Control System Using a Time-Dependent Adjoint Method". *Mathematical Modeling of Natural Phenomena, 6*(3), pp. 141–165.

[21] Lyness, J. N., 1967. "Numerical Algorithms Based on the Theory of Complex Variables". Proceedings of the ACM 22nd National Conference. Thomas Book Co., Washington, DC, pp. 124–134.

[22] Lyness, J. N., and Moler, C. B., 1967. "Numerical Differentiation of Analytic Functions". *SIAM Journal of Numerical Analysis, 4*(2), pp. 202–210.

[23] Squire, W., and Trapp, G., 1998. "Using Complex Variables to Estimate Derivatives of Real Functions". *SIAM Review, 10*(1), pp. 110–112.

[24] Newman, J. C., Anderson, W. K., and Whitfield, D. L., 1998. "Multidisciplinary Sensitivity Derivatives Using Complex Variables". MSSU-COE-ERC-98-08 (Mississippi State University).

[25] Newman, J. C., Anderson, W. K., and Whitfield, D. L., 1999. "A Step-Size Independent Approach for Multidisciplinary Sensitivity Analysis and Design Optimization". AIAA 1999-3101.

[26] DePauw, D., and Vanrolleghem, P.-A., 2005. "Using the Complex-Step Derivative Approximation Method to Calculate Local Sensitivity Functions of Highly Nonlinear Bioprocess Models". Proceedings of the 17th IMACS World Congress on Scientific Computation, Applied Mathematics, and Simulation. Paris, France.

[27] Perez-Foguet, A., Rodriguez-Ferran, A., and Huerta, A., 2000. "Numerical Differentiation for Local and Global Tangent Operators in Computational Plasticity". *Computer Methods in Applied Mechanics and Engineering, 189*(1), pp. 277–296.

[28] Butuk, N., and Pemba, J., 2003. "Computing CHEMKIN Sensitivities Using Complex Variables". *Journal of Engineering for Gas Turbines and Power, 125*(3), pp. 854–858.

[29] Gao, X.-W., and He, M.-C., 2005. "A New Inverse Analysis Approach for Multi-Region Heat Conduction BEM Using

Complex-Variable-Differentiation Method". *Engineering Analysis with Boundary Elements, 29*(8), pp. 788–795.

[30] Abokhodair, A., 2007. "Numerical Tools for Geoscience Computations: Semiautomatic Differentiation". *Computational Geosciences, 11*, pp. 283–296.

[31] Voorhees, A., Bagley, R., Millwater, H. R., and Golden, P., 2009. "Application of Complex Variable Methods for Fatigue Sensitivity Analysis". AIAA 2009-2711.

[32] Dennis, B. H., Jin, W., Dulikravich, G. S., and Jaric, J., 2011. "Application of the Finite Element Method to Inverse Problems in Solid Mechanics". *International Journal of Structural Changes in Solids, 3*(2), pp. 11–21.

[33] Kim, J., Bates, D. G., and Postlethwaite, I., 2006. "Nonlinear Robust Performance Analysis Using Complex-Step Gradient Approximation". *Automatica, 42*, pp. 177–182.

[34] Nielsen, E. J., and Anderson, W. K., 1999. "Aerodynamic Design Optimization on Unstructured Meshes Using the Navier-Stokes Equations". *AIAA Journal, 37*(11), pp. 1411–1419.

[35] Kleb, W. L., Nielsen, E. J., Gnoffo, P. A., Park, M. A., and Wood, W. A., 2004. "Collaborative Software Development in Support of Fast Adaptive AeroSpace Tools (FAAST)". AIAA 2004-2371.

[36] Nielsen, E. J., and Kleb, W. L., 2006. "Efficient Construction of Discrete Adjoint Operators on Unstructured Grids Using Complex Variables". *AIAA Journal, 44*(4), pp. 827–836.

[37] Shmilovich, A., and Yadlin, Y., 2009. "Active Flow control for Practical High-Lift Systems". *AIAA Journal of Aircraft, 46*(4), pp. 1354–1364.

[38] Nielsen, E. J., Diskin, B., and Yamaleev, N. K., 2010. "Discrete Adjoint-Based Design Optimization of Unsteady Turbulent Flows on Dynamic Unstructured Grids". *AIAA Journal, 48*(6), pp. 1195–1206.

[39] Rallabhandi, S. K., Nielsen, E. J., and Diskin, B., 2014. "Sonic-Boom Mitigation through Aircraft Design and Adjoint Methodology". *AIAA Journal of Aircraft, 51*(2), pp. 502–510.

[40] Park, M. A. "Anisotropic Output-Based Adaptation with Tetrahedral Cut Cells for Compressible Flows". PhD Thesis, Massachusetts Intitute of Technology, Cambridge, MA, September 2008.

[41] Heath, C. M., Gray, J. S., Park, M. A., Nielsen, E. J., and Carlson, J.-R., 2015. "Aerodynamic Shape Optimization of a Dual-Stream Supersonic Plug Nozzle". AIAA 2015-1047.

[42] Lorenz, E., 1963. "Deterministic Nonperiodic Flow". *Journal of the Atmospheric Sciences, 20*, pp. 130–141.

[43] Wang, Q., Hui, R., and Blonigan, P., 2014. "Least Squares Shadowing Sensitivity Analysis of Chaotic Limit Cycle Oscillations". *Journal of Computational Physics, 267*, pp. 210–224.

[44] Blonigan, P. J., Wang, Q., Nielsen, E. J., and Diskin, B., 2016. "Least Squares Shadowing Sensitivity Analysis of Chaotic Flow Around a Two-Dimensional Airfoil". AIAA 2016-0296.